Diverging seasonal extremes for ocean acidification during the twenty-first century

Lester Kwiatkowski, James C. Orr

Diverging seasonal extremes for ocean acidification during the twenty-first century

Lester Kwiatkowski[1*], James Orr[1]
Laboratoire des Sciences du Climat et de l'Environnement (LSCE), IPSL, CEA/CNRS/UVSQ, Orme des Merisiers, Gif-sur-Yvette, 91190, France.

*Lester Kwiatkowski
Laboratoire des Sciences du Climat et de l'Environnement (LSCE)
Orme des Merisiers
Gif-sur-Yvette
91190
France
Lester.Kwiatkowski@lsce.ipsl.fr

How ocean acidification will affect marine organisms depends on changes in both the long-term mean and the short-term temporal variability of carbonate chemistry[1,2,3,4,5,6,7,8]. While the decadal-to-centennial response to atmospheric CO_2 and climate change is constrained by observations and models[1,9], little is known about corresponding changes in seasonality[10,11,12], particularly for pH. Here we assess the latter by analysing 9 Earth System Models (ESMs) forced with a business-as-usual emissions scenario[13]. During the twenty-first century, the seasonal cycle of surface-ocean pH was attenuated by 16±7 %, on average, while that for hydrogen ion concentration $[H^+]$ was amplified by 81±16 %. Simultaneously, the seasonal amplitude of aragonite saturation state (Ω_{arag}) was attenuated except in the subtropics where it was amplified. These contrasting changes derive from regionally varying sensitivities of these variables to atmospheric CO_2 and climate change and diverging trends in seasonal extremes in the primary controlling variables (temperature, dissolved inorganic carbon, and alkalinity). Projected seasonality changes will tend to exacerbate impacts of increasing $[H^+]$ on marine organisms during summer and ameliorate impacts during winter, although the opposite holds in the high latitudes. Similarly over most of the ocean, impacts from declining Ω_{arag} are likely to be intensified during summer and dampened during winter.

Ocean CO_2 uptake affects marine chemistry via ocean acidification[1,9,14], a process that increases concentrations of CO_2, H^+ and HCO_3^-, and reduces levels of pH and CO_3^{2-}. Although much effort has been devoted to assessing the direct and indirect effects of increasing atmospheric CO_2 on the mean state of these ocean carbonate chemistry variables, few studies have addressed the corresponding changes in their seasonal cycles[10,11,12].

The seasonal cycles of ocean carbonate chemistry variables are the result of variations in the seasonality of different physical and biological processes[6,7]. Those for pCO_2 and pH are largely regulated by variations in temperature in the subtropics, while at higher latitudes their oscillations are typically dominated by biological uptake and release of CO_2 (photosynthesis and respiration). In contrast, temperature plays a minor role in controlling the seasonal cycles of the carbonate saturation state of seawater ($\Omega = [Ca^{2+}]\,[CO_3^{2-}]/K_{sp}$) even at lower latitudes; rather, it is the variability of total alkalinity and dissolved inorganic carbon that dominates[6,7].

To survive, marine organisms must cope with variations in their local environment, however many may be highly sensitive to changes in ocean carbonate chemistry[15,16]. Calcifying species such as echinoderms, byrozoans and cnidarians exhibit depressed calcification, growth and survival rates at lower $\Omega_{arag/calc}$ (refs. [3,4,15]). In teleost fish and marine invertebrates, ion exchange is reduced by extracellular acidosis or high external $[H^+]$, depressing protein synthesis and metabolic rates[17]. Physiological and behavioural functioning is also sensitive to pCO_2, with high external concentrations impairing olfactory discrimination[18] and predator-prey responses[19].

Accounting for seasonal variability in carbonate chemistry influences the timing of the projected onset of $CaCO_3$ undersaturation[10,11,20], when waters become corrosive to pure aragonite ($\Omega_{arag}<1$) and calcite ($\Omega_{calc}<1$) (i.e., metastable and stable forms of $CaCO_3$). These seasonal variations also affect when surface waters will reach a proposed threshold, beyond which pCO_2 levels may become damaging[12]. Here we explore how seasonality of surface-ocean $[H^+]$, pH and Ω_{arag} will respond to projected increases of atmospheric CO_2 and climate change during the twenty-first century. Unlike studies that have assumed unchanging seasonality, combining observational estimates of present seasonality (repeated in time) with model projections of the change in mean state[10,11], we use an ensemble of 9 Earth System Models (ESMs) containing coupled ocean biogeochemistry schemes. Thus we assess how seasonality is affected by increasing concentrations of atmospheric CO_2 and climate-change driven changes in sea surface temperature and biology[9,21].

Ocean biogeochemistry models (OBM) generally reproduce the amplitude and phase of observational estimates for seasonal air-sea CO_2 fluxes in the Pacific[22], Atlantic[23] and Indian Oceans[24] while their skill in high latitude regions is more limited[23,25,26]. We found consistent results for the CMIP5 ESMs that include an OBM. The models broadly capture the zonal-mean patterns of seasonal changes in $[H^+]$ ($r\sim0.8$) and Ω_{arag} ($r\sim0.95$) of observational climatologies (Supplementary Figs. 1-6). Hence they appear to offer the best option to assess projected changes in seasonality during the coming century. Nonetheless, model performance in the Southern Ocean is particularly limited, with certain models negatively correlated with the $[H^+]$ climatology, possibly due to excessive simulated warming in

summer[25] or underestimated winter convective CO_2 entrainment and the impact of biological CO_2 uptake[26].

Projected trends in seasonality were evaluated for the business-as-usual (2006-2100) Representative Concentration Pathway 8.5 (RCP8.5)[13] relative to results from the historical simulation[27] (1990-1999). Changes in seasonality were determined by subtracting a cubic spline fit from the monthly time series in each grid cell and calculating the annual peak-to-peak amplitude for each year of the detrended dataset. Both the mean state and seasonality of projected $[H^+]$, pH and Ω_{arag} change over the twenty-first century, as illustrated in Figure 1 for one model.

During this century, the amplitude of seasonal cycle in $[H^+]$ is projected to increase by 81±16 % (multi-model mean ± 1SD) (Fig. 2a). Increases in seasonal amplitudes of $[H^+]$ are generally higher in the high latitudes, particularly in the Arctic where the average amplification is 147±57 % (Fig. 3a, S8). Yet unlike the seasonal amplitude for $[H^+]$, that for pH is projected to decline globally, on average by 16±7 % during the twenty-first century (Fig.2b). Attenuation is generally more intense in the low and mid-latitudes but also occurs over most of the high-latitude ocean (Fig. 3b, S8). Given that pH is directly related to $[H^+]$, it is counterintuitive that while the seasonal amplitude in $[H^+]$ increases, the seasonal amplitude in pH declines. However, the log transformation implies that

$$d\,pH = \frac{-1}{2.303}\frac{d[H^+]}{[H^+]} \qquad (1)$$

That is, the seasonal amplitude of pH depends not only on the seasonal amplitude of $[H^+]$ but also on the annual mean $[H^+]$. For the seasonal amplitude in pH to remain constant in time, the relative change in the seasonal amplitude of $[H^+]$ would have to equal the relative change in annual mean $[H^+]$. Although the CMIP5 models project that the global mean, seasonal amplitude of $[H^+]$ increases by 81±16 % over the twenty-first century, the annual global mean $[H^+]$ simultaneously increases by 117±3 %. Hence their combination results in reduced seasonal amplitude of pH. In contrast, in the parts of the Arctic and Southern Ocean that exhibit increases in the seasonal amplitude of pH, the relative change in the seasonal amplitude of $[H^+]$ is larger than the relative change in the $[H^+]$ mean state. Yet in those regions, there is less agreement among models about the sign of these changes (Figs. 3b, S8).

Regarding Ω_{arag}, its global average seasonal amplitude is attenuated by 9±8 % during the twenty-first century (Fig. 3c). Attenuation can exceed 40 % in the temperate-to-polar zones, while in the subtropics, where the amplitude of the seasonal cycle of Ω_{arag} is much smaller (Supplementary Fig. 7), there is amplification of up to 30 % (Fig. 3c), as discussed below. These projected changes in the seasonal amplitude of $[H^+]$, pH and Ω_{arag} result from nonidentical changes in both the seasonal maxima and minima (Fig. 1, S12).

To further investigate the causes of changes in seasonal amplitudes of derived variables $[H^+]$ and Ω_{arag}, we used 2 complementary approaches: (1) idealised simulations and (2) first-order Taylor-series deconvolution. The idealised simulations partition the geochemical versus radiative effects of increasing atmospheric CO_2, where the geochemical effect is due to

ocean carbon uptake and the radiative effect influences carbonate chemistry through rising temperatures and simultaneous changes in marine biological activity. The deconvolution quantifies how the seasonal amplitude of each derived variable (Δy), is affected by changes in temperature (T), salinity (S), dissolved inorganic carbon (C_T) and total alkalinity (A_T), i.e., four model variables used to calculate carbonate chemistry. That is for y = $f(C_T, A_T, T, S)$,

$$\Delta y = \left(\frac{\partial y}{\partial C_T}\right)\Delta C_T + \left(\frac{\partial y}{\partial A_T}\right)\Delta A_T + \left(\frac{\partial y}{\partial T}\right)\Delta T + \left(\frac{\partial y}{\partial S}\right)\Delta S \qquad (2)$$

where the partial differentials are estimated numerically and ΔT, ΔC_T, ΔA_T and ΔS are the changes in input variables, synchronous with Δy, assuming other contributions are negligible. For the change in amplitude, Equation (2) is evaluated separately with decadal mean seasonal cycles for the first and last simulated decades of the RCP8.5 scenario, and then the latter is subtracted from the former.

This deconvolution illustrates how the proximate drivers of seasonal amplification of $[H^+]$ vary spatially. In the mid-to-high latitudes it is the residual effect of opposing increases in the terms for dissolved inorganic carbon ($(\partial H^+/\partial C_T)\Delta C_T$) and total alkalinity ($(\partial H^+/\partial A_T)\Delta A_T$) that dominates. However, in the low latitudes, changes in these two terms largely compensate, so it is the increase in the temperature term ($(\partial H^+/\partial T)\Delta T$) that dominates (Supplementary Fig. 9). Because the sensitivities of H^+ to C_T and A_T (partial differentials) are roughly equal and opposite, it is the balance between ΔC_T and ΔA_T that control the change in seasonal amplitude of $[H^+]$ in the mid-to high latitudes (Supplementary Fig. 10). One cannot assume that ΔA_T remains constant while only ΔC_T will change. For instance, changes in ΔA_T will be decoupled from those of ΔC_T due to an altered hydrological cycle. Increased freshwater input dilutes C_T and A_T, but C_T then tends to equilibrate with atmospheric CO_2, unlike A_T. Hence addition of low alkalinity freshwater reduces pH, despite the opposite tendency from dilution alone. The high latitudes will experience this effect most, from enhanced precipitation, ice melt, and river runoff. Decoupling will also result from anthropogenic CO_2 invasion and changes in primary production. In the low latitudes, while the C_T and A_T terms are small and compensating, the temperature term dominates, enhanced by a doubling of $\partial H^+/\partial T$ (Supplementary Fig. 11). The ultimate drivers of this seasonal amplification in $[H^+]$ are demonstrated by the idealised simulations, which show that it is the geochemical effect of increasing atmospheric CO_2 and consequently reduced buffer capacity[29,30] that is responsible for 92 % of global amplification, while the radiative effect provides minor reinforcement (Fig. 4, S13).

For Ω_{arag}, the proximate drivers of the general attenuation of its seasonal amplitude are a decline in the C_T term ($(\partial\Omega_{arag}/\partial C_T)\Delta C_T$) which typically outweighs an opposing increase in the A_T term ($(\partial\Omega_{arag}/\partial A_T)\Delta A_T$) (Supplementary Figs. 9-10). In the subtropics though, there is little change in the A_T term, while the C_T term increases due to a larger change in ΔC_T, driving amplification of the Ω_{arag} seasonal cycle in these regions. The ultimate driver of the seasonal attenuation in Ω_{arag} is the geochemical effect of increasing atmospheric CO_2 which is responsible for >100 % of global attenuation, being partly offset by the radiative effect (Fig. 4, S13). In contrast, the subtropical amplification of the seasonal cycle of Ω_{arag} results from the radiative effect driving enhanced amplification over the low latitudes in combination with the weaker attenuation from the geochemical effect in the subtropics.

We have shown that under a business-as-usual emissions scenario, the seasonal variability of ocean carbonate chemistry is projected to change substantially during this century. Despite the diversity of OBMs in the multi-model ensemble[9,21], spatial patterns of the change in seasonal amplitude of $[H^+]$, pH, and Ω_{arag} are generally consistent (Fig. 3, S8). Previously it was shown that increasing atmospheric CO_2 will amplify the seasonal cycle of surface-ocean pCO_2 (ref. [12]), potentially resulting in earlier exposure to detrimental pCO_2 conditions for marine organisms. Here we show that increasing atmospheric CO_2 must also amplify the seasonal cycle of $[H^+]$ in a similar manner. This is consistent with the near-linear relationship between $[H^+]$ and pCO_2 for annual-mean trends during the twenty-first century[31].

Amplified $[H^+]$ seasonality may worsen impacts from the long-term mean increase in $[H^+]$, potentially resulting in earlier seasonal exposure to conditions that cause physiological acidosis and depress protein synthesis and metabolic rates in marine organisms. In the low latitudes, this enhanced exposure is most likely to occur during summer when warming drives the $[H^+]$ seasonal high. In the high latitudes, enhanced exposure is most likely to occur when the effect of photosynthesis on $[H^+]$ drawdown is limited[6,7]. But amplified $[H^+]$ seasonality will also diminish exposure to conditions that cause acidosis during seasonal lows, e.g., in winter months in the low-latitudes and during phytoplankton blooms in the high-latitudes.

The seasonal amplitude of Ω_{arag} is projected to amplify in some regions and attenuate in others. Attenuation dominates throughout most of the ocean owing to increases in aqueous carbon dioxide $[CO_2^*]$, which reduces carbonate ion $[CO_3^{2-}]$ and hence the buffer capacity. In the subtropics though, the seasonal amplitude of Ω_{arag} increases because amplification driven by the radiative effect of CO_2 dominates the locally weak geochemical effect. The general attenuation of the seasonal amplitude of Ω_{arag} is likely to exacerbate the impact of declining Ω_{arag} during the summer high while dampening the impact of declining Ω_{arag} during the winter low.

The same processes that will affect future seasonal variability, particularly the direct geochemical effect from the atmospheric CO_2 increase and the corresponding indirect effect from radiative warming, are likely to affect future diurnal variability. Indeed we estimate an amplification of the diurnal cycle of $[H^+]$ (122%) and an attenuation of the diurnal cycle of Ω_{arag} (20%) that are similar to our estimates for the seasonal cycle, based on differences in observations of diel pH variability reported for two adjacent sites in the Bay of Naples, a control station and a station where natural venting of pure CO_2 has perturbed oceanic pCO_2 to reach levels expected for the late twenty-first century (Table S2; ref. [32]). Future research should assess how altered carbonate chemistry variability on both diurnal[33,34] and seasonal timescales will affect marine organisms, especially those suspected to be vulnerable to ocean acidification.

The diversity in projected changes in seasonal extremes of $[H^+]$, pH, Ω_{arag} and pCO_2 emphasizes the need to improve our understanding of the mechanisms that control how specific marine organisms are affected by ocean acidification. In particular, we will need to study the sensitivity of marine organisms to these simultaneous yet contrasting changes in seasonality to be able to assess aggregate effects on marine communities.

Figures

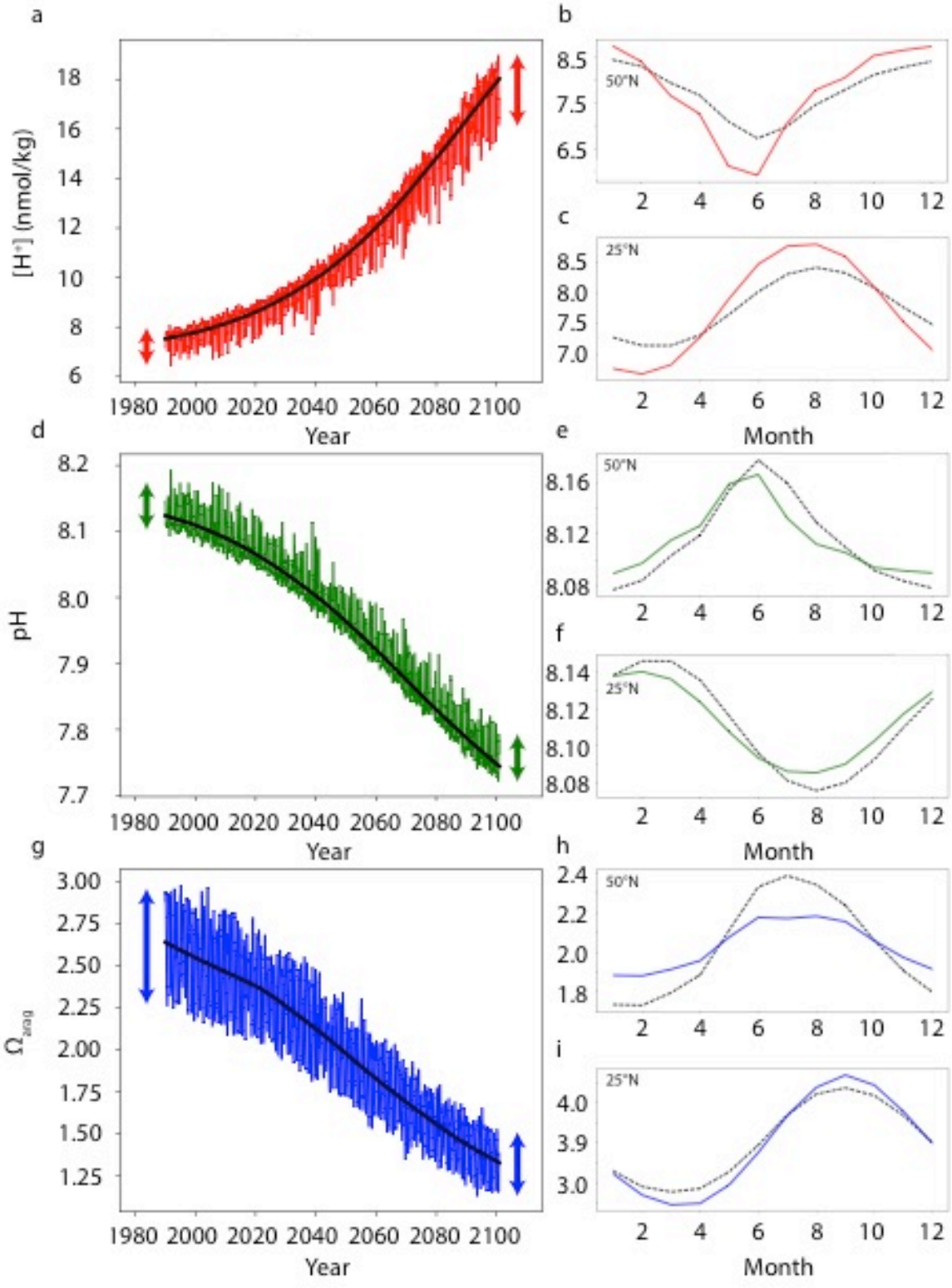

Figure 1. Changing seasonal cycles of carbonate chemistry variables. The projected **a-c**, $[H^+]$ **d-f**, pH and **g-i**, Ω_{arag} under the historical and RCP8.5 scenario of one CMIP5 model (MPI-ESM-LR). First column, monthly values and the long-term mean trend from an illustrative grid cell in the South Pacific (110°W, 40°S). Second column, the detrended zonal-mean seasonal cycles in the periods 1990-1999 (dashed) and 2090-2099 (line) at 25°N and 50°N.

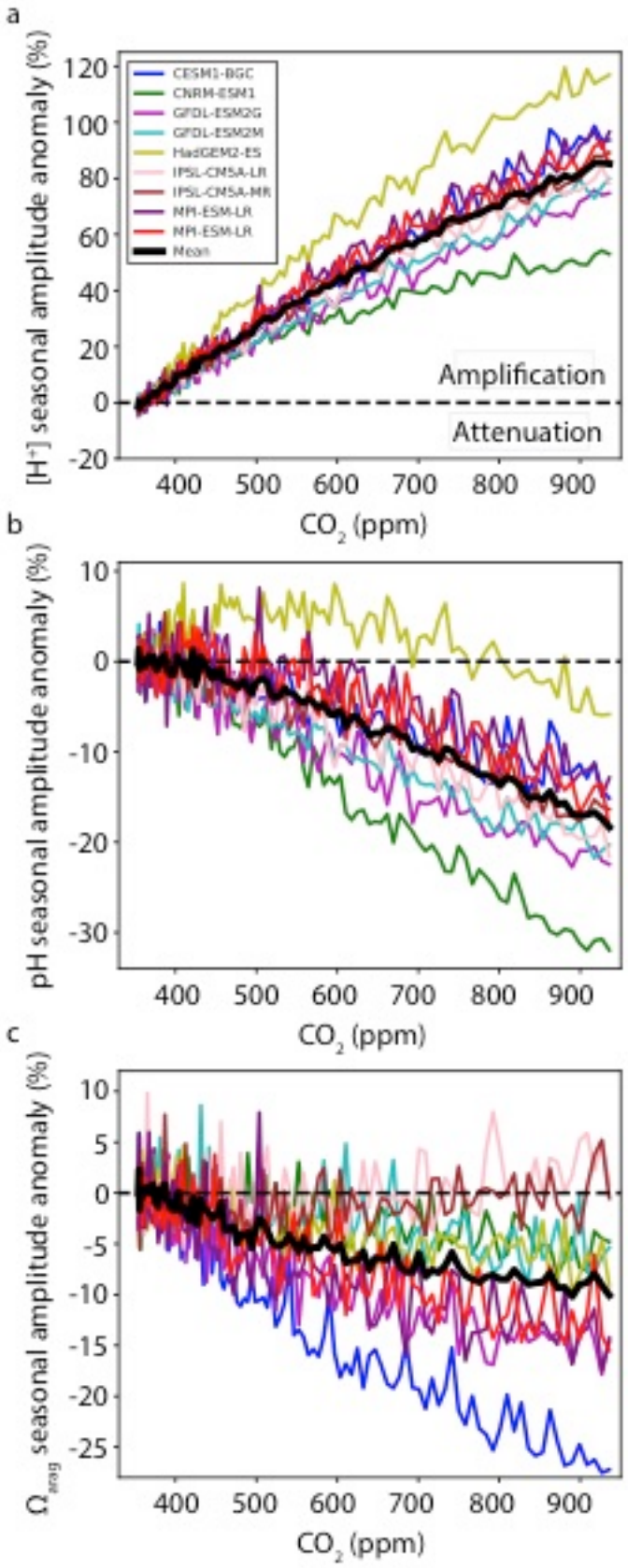

Figure 2. Relative change in the seasonal amplitude of carbonate chemistry variables with rising atmospheric CO_2. Global anomaly in the seasonal amplitudes of **a**, $[H^+]$ **b**, pH and **c**, Ω_{arag} relative to mean 1990s values as a function of atmospheric CO_2.

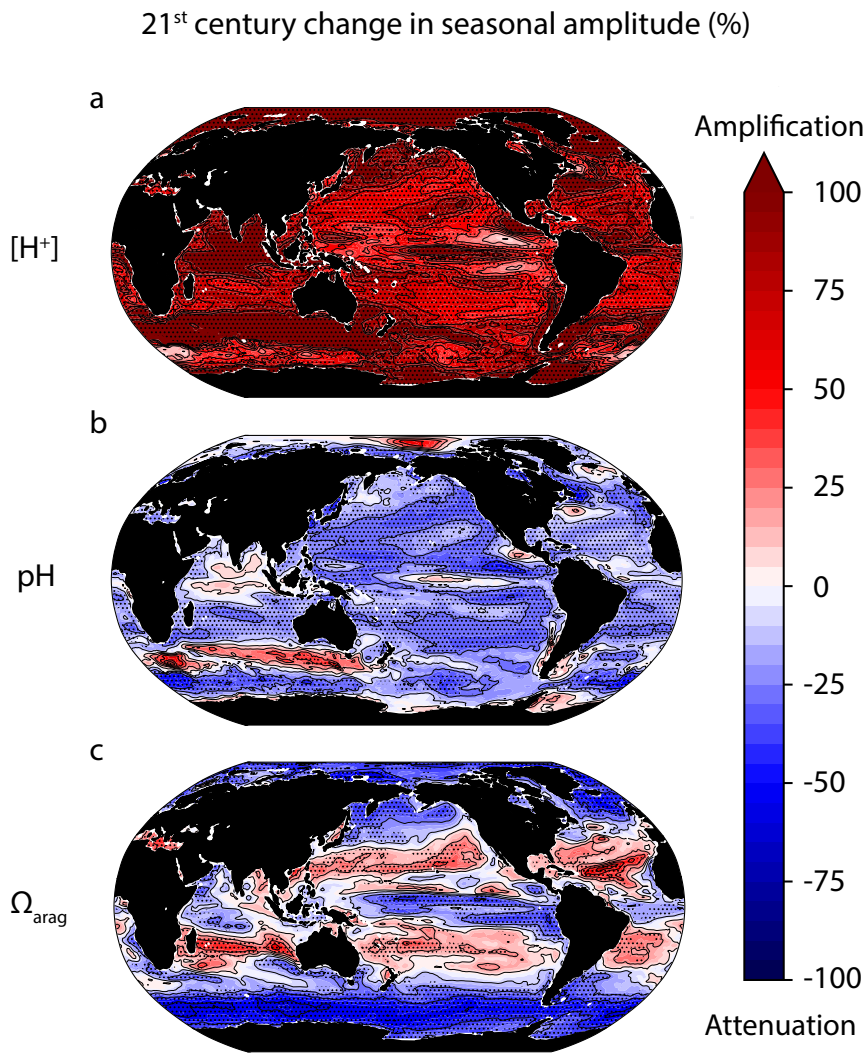

Figure 3. The twenty-first century changes in seasonal amplitudes. The model mean anomaly in the seasonal amplitude of **a**, $[H^+]$ **b**, pH and **c**, Ω_{arag} in the 2090s relative to the 1990s. Stippling shows areas of high confidence as determined by model sign agreement with a standard of 8 out of 9 models representing significance.

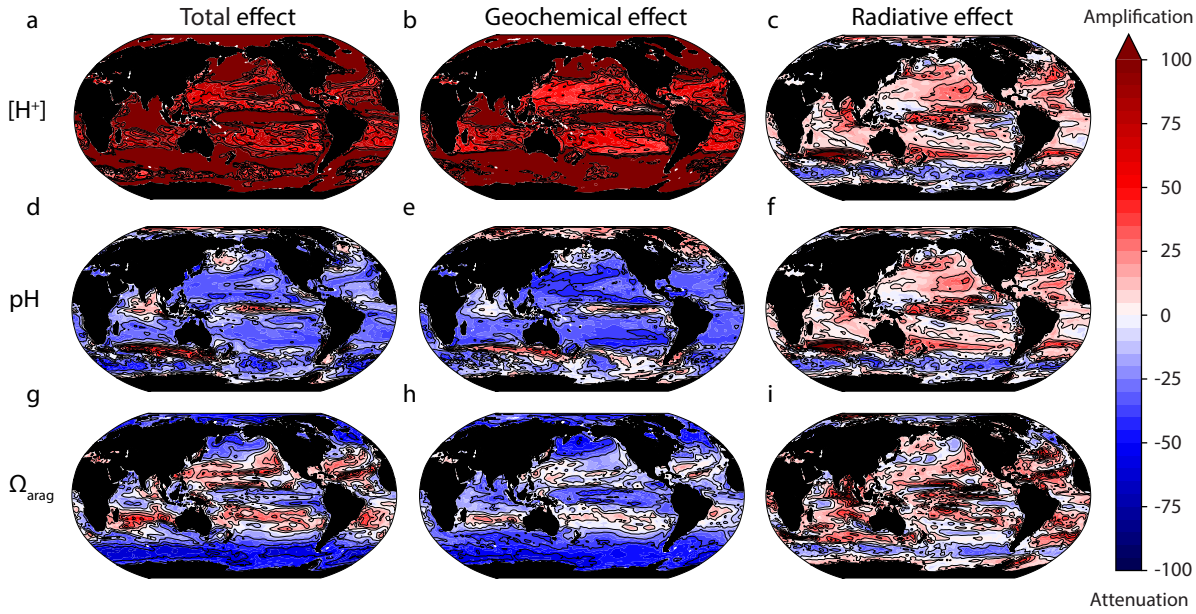

Figure 4. Partitioning of geochemical and radiative effects of atmospheric CO_2 on seasonality change. The model mean anomaly (%) in the seasonal amplitudes of **a-c**, $[H^+]$, **d-f**, pH and **g-i**, Ω_{arag} due to the geochemical, radiative and combined effect of atmospheric CO_2. Anomalies are calculated for the last decade of 4xCO2 simulations relative to the first decade.

References

1. Orr, J. C. *et al.* Anthropogenic ocean acidification over the twenty-first century and its impact on calcifying organisms. *Nature* **437,** 681–686 (2005).
2. Wootton, J. T., Pfister, C. A. & Forester, J. D. Dynamic patterns and ecological impacts of declining ocean pH in a high-resolution multi-year dataset. *Proc. Natl. Acad. Sci.* **105,** 18848–18853 (2008).
3. Albright, R. *et al.* Reversal of ocean acidification enhances net coral reef calcification. *Nature* **531,** 362–365 (2016).
4. Kwiatkowski, L. *et al.* Nighttime dissolution in a temperate coastal ocean ecosystem increases under acidification. *Sci. Rep.* **6,** 22984 (2016).
5. Shaw, E. C., McNeil, B. I., Tilbrook, B., Matear, R. & Bates, M. L. Anthropogenic changes to seawater buffer capacity combined with natural reef metabolism induce extreme future coral reef CO2 conditions. *Glob. Change Biol.* **19,** 1632–1641 (2013).
6. Takahashi, T. *et al.* Climatological distributions of pH, pCO2, total CO2, alkalinity, and CaCO3 saturation in the global surface ocean, and temporal changes at selected locations. *Mar. Chem.* **164,** 95–125 (2014).
7. Hagens, M. & Middelburg, J. J. Attributing seasonal pH variability in surface ocean waters to governing factors. *Geophys. Res. Lett.* **43,** 2016GL071719 (2016).
8. Takeshita, Y. *et al.* Including high-frequency variability in coastal ocean acidification projections. *Biogeosciences* **12,** 5853–5870 (2015).
9. Bopp, L. *et al.* Multiple stressors of ocean ecosystems in the 21st century: projections with CMIP5 models. *Biogeosciences* **10,** 6225–6245 (2013).
10. McNeil, B. I. & Matear, R. J. Southern Ocean acidification: A tipping point at 450-ppm atmospheric CO2. *Proc. Natl. Acad. Sci.* **105,** 18860–18864 (2008).
11. Sasse, T. P., McNeil, B. I., Matear, R. J. & Lenton, A. Quantifying the influence of CO2 seasonality on future aragonite undersaturation onset. *Biogeosciences* **12,** 6017–6031 (2015).
12. McNeil, B. I. & Sasse, T. P. Future ocean hypercapnia driven by anthropogenic amplification of the natural CO2 cycle. *Nature* **529,** 383–386 (2016).
13. Riahi, K. *et al.* RCP 8.5—A scenario of comparatively high greenhouse gas emissions. *Clim. Change* **109,** 33–57 (2011).
14. Doney, S. C., Fabry, V. J., Feely, R. A. & Kleypas, J. A. Ocean Acidification: The Other CO2 Problem. *Annu. Rev. Mar. Sci.* **1,** 169–192 (2009).
15. Kroeker, K. J., Kordas, R. L., Crim, R. N. & Singh, G. G. Meta-analysis reveals negative yet variable effects of ocean acidification on marine organisms. *Ecol. Lett.* **13,** 1419–1434 (2010).
16. Mangan, S., Urbina, M. A., Findlay, H. S., Wilson, R. W. & Lewis, C. Fluctuating seawater pH/pCO2 regimes are more energetically expensive than static pH/pCO2 levels in the mussel Mytilus edulis. *Proc R Soc B* **284,** 20171642 (2017).
17. Pörtner, H.-O. Ecosystem effects of ocean acidification in times of ocean warming: a physiologists view. *Mar. Ecol. Prog. Ser.* **373,** 203–217 (2008).
18. Munday, P. L. *et al.* Ocean acidification impairs olfactory discrimination and homing ability of a marine fish. *Proc. Natl. Acad. Sci.* **106,** 1848–1852 (2009).
19. Watson, S.-A., Fields, J. B. & Munday, P. L. Ocean acidification alters predator behaviour and reduces predation rate. *Biol. Lett.* **13,** 20160797 (2017).
20. Gruber, N. *et al.* Rapid Progression of Ocean Acidification in the California Current

System. *Science* **337,** 220–223 (2012).
21. Kwiatkowski, L. *et al.* Emergent constraints on projections of declining primary production in the tropical oceans. *Nat. Clim. Change* **7,** 355–358 (2017).
22. Ishii, M. *et al.* Air–sea CO2 flux in the Pacific Ocean for the period 1990–2009. *Biogeosciences* **11,** 709–734 (2014).
23. Schuster, U. *et al.* An assessment of the Atlantic and Arctic sea–air CO2 fluxes, 1990–2009. *Biogeosciences* **10,** 607–627 (2013).
24. Sarma, V. V. S. S. *et al.* Sea–air CO2 fluxes in the Indian Ocean between 1990 and 2009. *Biogeosciences* **10,** 7035–7052 (2013).
25. Lenton, A. *et al.* Sea–air CO_2 fluxes in the Southern Ocean for the period 1990–2009. *Biogeosciences* **10,** 4037–4054 (2013).
26. Mongwe, N. P., Chang, N. & Monteiro, P. M. S. The seasonal cycle as a mode to diagnose biases in modelled CO2 fluxes in the Southern Ocean. *Ocean Model.* **106,** 90–103 (2016).
27. Taylor, K. E., Stouffer, R. J. & Meehl, G. A. An Overview of CMIP5 and the Experiment Design. *Bull. Am. Meteorol. Soc.* **93,** 485–498 (2011).
28. Rodgers, K. B. *et al.* A wintertime uptake window for anthropogenic CO2 in the North Pacific. *Glob. Biogeochem. Cycles* **22,** GB2020 (2008).
29. Egleston, E. S., Sabine, C. L. & Morel, F. M. M. Revelle revisited: Buffer factors that quantify the response of ocean chemistry to changes in DIC and alkalinity. *Glob. Biogeochem. Cycles* **24,** GB1002 (2010).
30. Hauck, J. & Völker, C. Rising atmospheric CO2 leads to large impact of biology on Southern Ocean CO2 uptake via changes of the Revelle factor. *Geophys. Res. Lett.* **42,** 2015GL063070 (2015).
31. Orr, J. C. Recent and future changes in ocean carbonate chemistry. in *Ocean acidification* **1,** 41–66 (2011).
32. Kerrison, P., Hall-Spencer, J. M., Suggett, D. J., Hepburn, L. J. & Steinke, M. Assessment of pH variability at a coastal CO2 vent for ocean acidification studies. *Estuar. Coast. Shelf Sci.* **94,** 129–137 (2011).
33. Schulz, K. G. & Riebesell, U. Diurnal changes in seawater carbonate chemistry speciation at increasing atmospheric carbon dioxide. *Mar. Biol.* **160,** 1889–1899 (2013).
34. Jury, C. P., Thomas, F. I. M., Atkinson, M. J. & Toonen, R. J. Buffer Capacity, Ecosystem Feedbacks, and Seawater Chemistry under Global Change. *Water* **5,** 1303–1325 (2013).

Acknowledgements

This study was funded by the H2020 CRESCENDO grant (ref 641816) and the ERC IMBALANCE-P synergy grant (ref 610028). We acknowledge the World Climate Research Programme's Working Group on Coupled Modelling, which is responsible for CMIP. For CMIP the US Department of Energy's Program for Climate Model Diagnosis and Intercomparison provided coordinating support and led the development of software infrastructure in partnership with the Global Organisation for Earth System Science Portals. To analyse the CMIP5 data, this study benefited from the IPSL Prodiguer-Ciclad facility, which is supported by CNRS, UPMC, Labex L-IPSL which is funded by the ANR (ref ANR-10-LABX-0018) and by the European FP7 IS-ENES2 project (ref 312979). We thank B. Le Vu for preliminary discussions.

Author contributions

Both authors conceived this study, J.O. produced the derived variables, and both authors performed the analysis and wrote the manuscript, with L.K. leading the process.

Additional information

Correspondence and requests for materials should be addressed to L.K.

Competing financial interests

The authors declare no competing financial interests

Methods

Earth System Models

Monthly surface-ocean carbonate chemistry fields were computed from monthly output of 9 CMIP5 models (Table S1) from prognostic fields for total alkalinity, dissolved inorganic carbon, temperature, salinity, and total dissolved inorganic phosphorus and silicon. Calculations were made offline using the *mocsy* package and the equilibrium constants recommended for best practices[35]. Output fields were regridded to a regular 1° x 1° regular grid to facilitate multi-model intercomparison. All quoted error bars represent one standard deviation of the multi-model mean.

Model evaluation

CMIP5 seasonal climatologies constructed from 1995-2004 model output years were compared against the Takahashi et al., 2014 (ref. [6]) observational climatologies of $[H^+]$, pH, pCO_2 and Ω_{arag} (Supplementary Figs. 1-6). Model output was regridded to the Takahashi 4° x 5° grid with the same ocean mask applied. The models generally capture the zonal-mean patterns of seasonality for observed climatologies of $[H^+]$, pH, pCO_2 and Ω_{arag}. The multi-model ensemble encompasses the observed seasonal variance for Ω_{arag} yet overestimates the seasonal variance of $[H^+]$ and pCO_2 (Supplementary Figs. 1-2). This overestimation is driven by the zonal-mean component of seasonal variance (Supplementary Figs. 1-2). Across all carbonate chemistry variables, models have high correlation coefficients for the zonal-mean component of seasonal variability and relatively low correlation coefficients for the zonal-anomaly component of seasonal variability. Model performance is generally best in the subtropics and worst in the Southern Ocean with respect to both $[H^+]$ and Ω_{arag} (Supplementary Figs. 3-6). Yet in the Southern Ocean, the data used to construct the climatologies are typically summer biased.

Idealised simulations

Three out of the 9 models also ran idealised simulations that allowed us to separate the geochemical effect from the CO_2 increase from the radiative forcing effect of the same CO_2 increase. More precisely, we used results from three CMIP5 experiments: 1pctCO2, esmFixClim1 and esmFdbk1. Although these simulations are not directly comparable to those with the RCP8.5 scenario due to different simulation lengths and atmospheric CO_2 concentrations, they provide the only means of separating the ultimate geochemical and radiative drivers of seasonality change. In the 1pctCO2 simulations, the atmospheric CO_2 concentration increases from 280 ppm by 1 % per year reaching a doubling ($2xCO_2$) after 70 years (560 ppm) and quadrupling ($4xCO_2$) after 140 years. In the esmFixClim1 simulations, the atmospheric CO_2 concentration follows that of the 1pctCO2 simulations while the radiative module of each model experiences a constant atmospheric CO_2 concentration of 280 ppm. Conversely, in the esmFdbk1 simulations, the atmospheric CO_2 concentration is held constant at 280 ppm but the radiative module of each model experiences the same CO_2 concentration as the 1pctCO2 simulations. The mean response of the models in the 1pctCO2 simulations is similar spatially to that of the multi-model ensemble in RCP8.5 simulations (Figs. 3, 4). This confirms that atmospheric CO_2 emissions are the driver of patterns of

carbonate chemistry seasonality change and validates the use of the esmFixClim1 and esmFdbk1 simulations to partition the radiative and geochemical influences of CO_2. It should be noted that there are limited increases in ocean temperatures in the esmFixClim1 simulations that result from changes associated with the terrestrial biosphere, for which elevated CO_2 reduces stomatal conductance, which in turn drives greater surface sensible heat fluxes and thus slight increases in temperatures[36].

Taylor-series deconvolution

The first-order Taylor-series deconvolution was performed for $[H^+]$ and Ω_{arag} independently with output from the RCP8.5 simulations (eqn. 2). The partial differential terms were estimated numerically using the *mocsy* package and ΔT, ΔC_T, ΔA_T and ΔS represent the change in input variables synchronous with Δy. This approach reproduces the changes in the seasonal amplitude of each of the derived variables $[H^+]$ and Ω_{arag} to within much less than 1 % as shown in Figure S9. With the exception of the very high latitudes, the deconvolution was broadly consistent across the multi-model ensemble. The zonal-mean influence of the different terms is given in the supplementary material for the representative GFDL-ESM2M model (Supplementary Figs. 9-11).

Data availability

All the CMIP5 ESM model data are available via the Earth System Grid Federation (ESGF). The derived data that support the findings of this study are available from the corresponding author upon request.

References

35. Dickson, A. G., Sabine, C. L. & Christian, J. R. Guide to Best Practices for Ocean CO2 Measurements. (North Pacific Marine Science Organization, 2007).

36. Sellers, P. J. *et al.* Comparison of Radiative and Physiological Effects of Doubled Atmospheric CO2 on Climate. *Science* **271,** 1402–1406 (1996).